0038-075C/02/16705-303–314
Soil Science

May 2002
Vol. 167, No. 5
Printed in U.S.A.

TECHNICAL ARTICLES

RESIDENCE TIME EFFECTS ON ARSENATE SURFACE SPECIATION AT THE ALUMINUM OXIDE-WATER INTERFACE

Yuji Arai and D.L. Sparks

Bioavailability of metals/metalloids is often rate limited by contact time (i.e., residence time) in soils and sediments, resulting in irreversible reactions. The fate and transport of the contaminants must be predicted/modeled not only on short-term (<48 h) adsorption/desorption studies but also on long-term (months-years) reactions. However, there is very little information on the long-term effects of metal/metalloid partitioning reactions in soils and soil components. In this study, residence time effects (3 days–1 yr) on As(V) adsorption/desorption reactions and on As(V) surface speciation at the aluminum oxide-water interface were investigated using batch adsorption/desorption experiments coupled with time-resolved Extended X-ray Absorption Fine Structure spectroscopy (EXAFS). Biphasic As(V) adsorption kinetics were observed at pH 4.5 and 7.8, and whereas the reaction at pH 4.5 was nearly completed after 3 days, slow adsorption continued at pH 7.8 after 1 year. The longer the residence time (3 days–1 yr), the greater the decrease in As(V) desorption at both pHs, suggesting nonsingular reactions. EXAFS analyses on aged As(V) reacted aluminum oxide at both pHs showed that As-Al interatomic distances were 3.11 − 3.14 Å (±0.13 Å) in all of the aged samples (3 days to 1 yr) at pH 4.5 and 7.8, suggesting that predominantly bidentate binuclear bonding environments were present. As a point of interest, X-ray Absorption Near Edge Structure spectroscopy (XANES) features suggested some changes in the local chemical structure of adsorbed As(V) with aging. The surface transformations such as (i) a rearrangement of surface complexes and/or (ii) a conversion of surface complexes into aluminum arsenate-like precipitates might be important chemical factors responsible for the decrease in As(V) reversibility with aging. (Soil Science 2002;167:303–314)

Key words: Arsenate, adsorption, desorption, residence time, kinetics, surface speciation, surface precipitation, aluminum oxide, EXAFS.

SOILS and sediments are nearly always at disequilibrium with respect to ion transformations (Sparks, 1987). The rate of bioavailability of contaminants in the environment can be reduced with increasing time (Pignatello and Xing, 1995). The observation that less sorbate is released with increasing contact time between the sorbent and sorbate is referred to as a residence time/aging effect (Pignatello and Xing, 1995; Sparks, 1995). Even in the absence of a residence time effect, one often observes biphasic reaction processes for both sorption and desorption of metals, metalloids, and organic chemicals (Sparks, 1989). The biphasic behavior is characterized by a relatively rapid reaction followed by a slow reaction(s). The slow reactions have been ascribed to diffusion phenomena, differing sites of reactivity, and surface precipitation (Scheidegger et al., 1996); how-

Department of Plant and Soil Sciences, University of Delaware, Newark, DE 19717-1303. Dr. Arai is corresponding author. E-mail: ugarai@udel.edu

Received Aug. 28, 2001; accepted Jan. 10, 2002.

ever, without molecular scale investigations, the mechanism for sorption/desorption reactions cannot be verified.

Several *in situ* spectroscopic studies (Extended X-ray Absorption Fine Structure spectroscopy (EXAFS), Attenuated total reflectance Fourier Transform infrared (ATR-FTIR) spectroscopy, and Raman spectroscopy) have shown different metal/metalloid chemical speciation at metal oxide/phyllosilicate-water interfaces. The formation of outer-sphere selenate complexes (Hayes et al., 1987), a mixture of inner-sphere and outer-sphere As(III), Co(II), and Pb(II) complexes (Arai et al., 2001; Papelis and Hayes, 1996; Strawn et al., 1998), inner-sphere As(III and V), Cu(II), Pb(II), and Zn(II) surface complexes (Arai et al., 2001; Bargar et al., 1997; Cheah et al., 1998; Fendorf et al., 1997; Goldberg and Johnston, 2001; O'Reilly et al., 2001; Waychunas et al., 1993), and mixed metal (Ni(II) and Zn(II))-aluminum surface precipitates (Ford and Sparks, 2000; Scheidegger et al., 1997) have been determined. However, although many spectroscopic studies have provided important information on chemical speciation for reaction processes of more than 48 hours, the mechanisms for longer reaction times (days to months) have not been investigated extensively. Changes in the surface speciation of Co(II)/Ni(II)-Al surface precipitates on kaolinite and pyrophyllite were reported for 1 to several month(s) of reaction time (Ford et al., 1999; O'Day et al., 1994; Scheckel et al., 2000; Thompson et al., 1999). Some researchers have shown that metals/metalloids (i.e., As(V), Ni(II), and Pb(II)) reacted with metal oxides and pyrophyllite over longer times resulted in either irreversible or reversible retention mechanisms (Ford et al., 1999; O'Reilly et al., 2001; Strawn et al., 1998). For example, with 1 year aged Ni(II) reacted pyrophyllite, there was little Ni(II) release by HNO_3 and EDTA (Ford et al., 1999; Scheckel et al., 2000). Conversely, O'Reilly et al. (2001) found that 200 days aging time did not cause a decrease in As(V) release from aged As(V) reacted goethite samples when phosphate was the desorbing ligand (O'Reilly et al., 2001). Accordingly, long-term metal/metalloid ion partitioning reactions can/cannot become significant factors in controlling the contaminant bioavailability in soils and sediments.

In this study, we investigated the effect of residence time (3 days to 1 yr) on As(V) surface speciation at the aluminum-oxide water interface. To understand better the chemical processes responsible for the residence time effect, macroscopic batch adsorption/desorption experiments were coupled with molecular scale time-resolved EXAFS analysis. Arsenate, derived from indigenous sources and anthropogenic inputs, was chosen as the adsorbate because it is a toxic metalloid in oxic terrestrial water environments The impact of As on human/ecological health is cause for great concern in the United States (Allen et al., 1995). Interest in As has recently been heightened by the controversy over setting the maximum concentration level of As in drinking water, which was recently set at 10 ppb (USEPA, 2001). Aluminum oxide was chosen as an adsorbent because (i) it is a common soil mineral that has high adsorption capacity for various oxyanions (e.g., arsenate) and (ii) it is a potential adsorbent (e.g., activated alumina) for As at water treatment plants.

MATERIALS AND METHODS

Materials

The γ-Al_2O_3 (Degussa Inc., Akron, OH) was chosen as an adsorbate because well hydrated γ-Al_2O_3 (bayerite polymorph) contains aluminum octahedral sheets similar to aluminum oxides in soils (e.g., gibbsite) (Dyer et al., 1993; Wijnja and Schulthess, 1999). Total ignition and transmission electron microscopic analyses showed greater than 99.6% purity and an average particle radius of 13 nm (Degussa Inc., Akron, OH). The 5-point Brunauer-Emmett-Teller surface area was 90.1 ($\pm$ 0.2) $m^2\ g^{-1}$. The isoelectric point was 9.3 ($\pm$ 0.1), as determined by electrophoretic mobility measurements (Arai et al., 2001). ACS grade sodium arsenate, $Na_2HAsO_4 \cdot 7H_2O$ (Baker) and NaCl (Fisher) were used as reagent sources. A mansfieldite ($Al_2O_3 \cdot AsO_5 \cdot 4H_2O$, South Bedford mining, Gawton, near River Tamar, England) was used in the EXAFS analyses to extract theoretical phases-shift and amplitude reduction factors using the structural refinement data and the ab initio computer code FEFF702. The mansfieldite contains a corner-sharing three-dimensional network of *cis*-$AlO_4 \cdot 2H_2O$ octahedra and AsO_4 tetrahedra strucures similar to other members of the variscite group such as scorodite ($FeAsO_4 \cdot 2H_2O$).

Methods

Batch Adsorption Experiments

The adsorption kinetic experiments were performed in two steps. First, the γ-Al_2O_3 suspension (5g L^{-1}) was hydrated in 200 mL of 0.1*M* NaCl background electrolyte solutions for approximately 1 month. This hydration time was employed to assure the transformation of γ-

Al_2O_3 into a bayerite polymorph, hereafter referred to as aluminum oxide (Dyer et al., 1993; Wijnja and Schulthess, 1999). Second, the pH of the mineral suspensions was adjusted to pH 4.5 and 7.8 for 24 h using a stirred pH-stat apparatus, and these pHs were maintained during the first 48 h of the kinetic experiments as described below. The MINEQL+ chemical speciation program predicted that the experimental systems were undersaturated with respect to boehmite, gibbsite, and amorphous Al_2O_3 during hydration and pH adjustments. Fifty milliliters of a 5 m*M* sodium arsenate stock solution (5 m*M* sodium arsenate and 0.1 *M* NaCl) were added slowly (10 mL additions every 30 s) to assure an initial As(V) concentration of 1 m*M*. The mineral suspensions were stirred at 300 r.p.m. at 298 K. Samples (10 mL) of the mineral suspensions were taken periodically (at 5, 15, and 30 min and 1, 2, 4, 6, 12, and 24 h) and then passed through a 0.2-μm Gelman Supor®-200 membrane filter (Pall Corp., Ann Arbor, MI). The filtrates were analyzed for total As and Al by ICP-AES and or dissolved As(V) by the colorimetric method described by Cummings et al. (Cummings et al., 1999). After 48 h of reaction using the pH-stat apparatus, the reaction vessels were placed on an orbital shaker and shaken continuously at 300 r.p.m. for up to 12 months. pH was adjusted manually every 15 to 30 days with the addition of 0.1 *M* HCl or 0.1 *M* NaOH over the adsorption reaction period of 48 hours to 12 months. As(V) uptake from the bulk solution was monitored continuously at 5 and 15 days and 1, 4.5, 7, and 12 months. Total As in the filtrate was analyzed using the methods described above.

Batch Desorption Experiments

Arsenate reversibility from aged (3 days and 1, 4.5, and 12 months) As(V) reacted aluminum oxide samples at pH 4.5 and 7.8 was investigated using a replenishment technique. The replenishment method was chosen over a flow-method (e.g., miscible displacement and stirred flow methods) because the fine particle size of the γ-Al_2O_3 (average particle radius of 13 nm, Degussa Inc., Akron, OH) caused clogging of the filter when flow-methods were used. The aged samples were prepared according to the method described in the previous section. Thirty milliliters of duplicate aged suspensions were transferred into 50 mL polycarbonate high-speed centrifuge tubes and were centrifuged at 11,950 g for 10 min. The supernatant was decanted to recover the paste. The samples were resuspended in 30 mL of desorption solutions containing 0.096 *M* NaCl, 1 m*M* sodium sulfate, and 2 m*M* organic buffer (sodium acetate (Na-Ac) or 4-(2-hydroxyethyl)-1-piperazine-ethanesulfonic acid (HEPS). The organic buffers Na-Ac and HEPS were used to maintain pH (i.e., 4.5 and 7.8 ± 0.2, respectively) during the desorption experiments. Tubes were shaken at 300 r.p.m. at 298 K for 24 h. The suspensions were then centrifuged, and the supernatant was analyzed for As(V) using the methods described in the adsorption kinetics section. The replenishment procedure was repeated 25 times (i.e., 25 days).

Arsenic K Edge EXAFS Analysis

XAS samples (3 days and 4, 7, and 11 months at pH 4.5 and 3 days and 1, 8, and 12 months at pH 7.8) were prepared according to the methods described in the adsorption kinetics section above. Paste samples were recovered by centrifuging 30 mL of As(V) reacted aluminum oxide suspensions in 50 mL polycarbonate high-speed centrifuge tubes at 11,950 *g* for 10 min, and the supernatant was decanted. All paste samples were loaded on openings (70 mm × 250 mm) of Teflon sample holders (250 mm × 400 mm), and the openings were sealed with a Type K-104 Kapton tape (E.I. Dupont, Wilmington, DE). Arsenic K-edge (11867 eV) XAS spectra were collected on beamline X-11A at the National Synchrotron Light Source (NSLS), Brookhaven National Laboratory, Upton, New York. The electron storage ring was operated at 2.528 GeV with a current range of 130 to 300 mA. The XAS spectra were collected in fluorescence mode with a Lytle detector filled with krypton gas. The ionization chamber (I_o) was filled with 90% N_2 and 10% Ar. As an internal standard, the arsenic K-edge of sodium arsenate salt (1% by weight in boron nitride) was run simultaneously with adsorption samples to check for potential energy shifts during the run. A Ge-filter was used to remove elastically scattered radiation from the fluorescence emissions. The monochromator consisted of two parallel Si(111) crystals with a vertical entrance slit of 0.5 mm. The Teflon sample holder was oriented at 45° to the unfocused incident beam. All samples were scanned at 298 K. A total of three to four spectra were collected for the adsorption samples, and one spectrum was collected for reference minerals such as mansfieldite, which was diluted to 1% by weight in ACS grade boron nitride for the XAS measurements.

XAS data reduction and analysis were performed using WinXas 2.0 (Ressler, 1997) using the following procedures. First, three spectra per sample were averaged. The averaged spectra were

normalized with respect to E_o determined from the second derivative of the raw spectra, and the total atomic cross sectional absorption was then set to unity. A low-order polynomial function was fit to the pre-edge region and the postedge region. Next, the data were converted from E-space to *k*-space and weighted by k^3 to compensate for dampening of the XAFS amplitude with increasing *k* space. Fourier transformation was then performed over the *k*-space range of 1.8 to 11.6 $Å^{-1}$ to obtain the radial structural functions (RSF). Final fitting of the spectra was done on Fourier transformed k^3 weighted spectra in R-space. The FEFF702 code reference (Zabinsky et al., 1995) was utilized to calculate single scattering theoretical spectra and phase shifts for As-O and As-Al backscatters using an input file based on the structural refinement of mansfieldite ($AlAsO_4 \cdot 2H_2O$). During fitting, the values of N and R of the As-O and As-Al shells were allowed to vary, as was a single E_0 for all sets of backscattering atoms. The Debye-Waller factors of the As-O shells were also allowed to vary, but those of the As-Al shells were fixed at 0.006 $Å^2$. When allowed to vary, the Debeye-Waller factors of the As-Al shells showed no trends for different aged samples, and we therefore used the average values (i.e., 0.006 $Å^2$) in the final fitting procedure to reduce the number of free parameters.

RESULTS AND DISCUSSION

Arsenate Adsorption Kinetics

Arsenate adsorption kinetics at the aluminum oxide-water interface at pH 4.5 and 7.8 are shown in Fig. 1. The initial fast adsorption was followed by a continuous slow adsorption with increasing time at both pHs. A similar biphasic reaction phenomenon has been well documented for tetrahedral oxyanion (i.e., phosphate and arsenate) reactions on soils and soil components (i.e., amorphous $Al(OH)_3$, natural allophane, ferrihydrite, hematite, goethite, α-Al_2O_3, and kaolinite) over different time scales (hours to months) (Anderson et al., 1976; Barron and Torrent, 1995; Barrow, 1974; Barrow, 1985; Beek and van Riemsdijk, 1982; Black, 1942; Colemann, 1944; Edzwald et al., 1976; Fuller et al., 1993; Hingston et al., 1974; Hsu and Rennie, 1962; Kafkafi et al., 1967; Madrid and Posner, 1979; Okajima et al., 1983; O'Reilly et al., 2001; Parfitt, 1979; Parfitt, 1989; Ryden et al., 1977; van Riemsdijk et al., 1977; Willett et al., 1988). Although As(V) adsorption at pH 4.5 was nearly completed after 750 h, only 46% of total As(V) uptake was achieved at pH 7.8, and the reaction continued after 1 yr (8640 h).

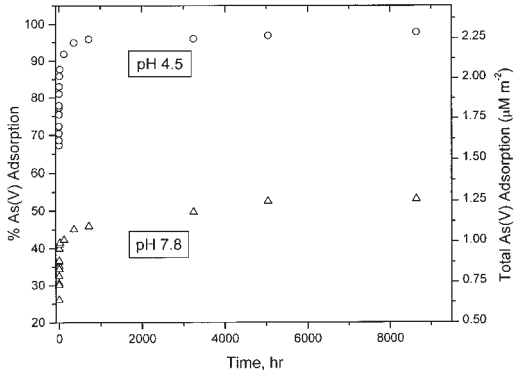

Fig. 1. Arsenate adsorption kinetics at the aluminum oxide-water interface at pH 4.5 and 7.8.

The difference in the kinetics at the two pHs could be explained by differences in the surface charge density of the aluminum oxide at the experimental pHs (4.5 and 7.8). The dissociation constants of H_3AsO_4 (pK_1 2.20, pK_2 6.97, and pK_3 13.4) indicate that the predominant As(V) solution speciation consisted of negatively charged species at our experimental pHs (i.e., $H_2AsO_4^-$ at pH 4.5 and $HAsO_4^{2-}$ at pH 7.8) (Schecher and McAvoy, 1998). The surface charge density of the aluminum oxide becomes more negatively charged with increasing pH_{bulk} from 4.5 to the IEP of the solid (≈9.3) (Arai et al., 2001). Therefore, the mineral surface at pH 4.5 is more positively charged than at pH 7.8, and the protonated mineral surfaces at pH 4.5 may have a strong attraction for negatively charged As(V) solution species (e.g., $H_2AsO_4^-$). Our macroscopic evidence that negatively charged As solution species significantly sorbed onto positively charged aluminum oxide surfaces over time suggest possibilities for both electrostatic interaction and ligand exchange mechanisms. However, previous electrophoretic mobility measurements have shown that formation of As(V) inner-sphere surface complexes at the aluminum oxide-water interface are caused by shifts in the electrophoretic mobility of aluminum oxide particles after As(V) adsorption (Arai et al., 2001; Suarez et al., 1999). In addition, our previous EXAFS study (Arai et al., 2001) and the *in situ* vibrational spectroscopic study of Goldberg and Johnston (2001) show that the formation of inner-sphere complexes via ligand exchange was predominantly responsible for As(V) adsorption (<48 h) at the aluminum oxide-water interface.

Differences in the initial (<48 h) adsorption kinetics at pH 4.5 and 7.8 might be attributed largely to the charge property of the mineral surface and the adsorbate solution speciation discussed above. However, the chemical factors responsible for the slow As(V) adsorption kinetics after 48 h are difficult to determine if based on the macroscopic data alone because changes in the charge properties of the mineral surface, the surface area, and the aluminum oxide structure are probably occurring with aging. Therefore, we used the EXAFS technique to investigate the changes in As(V) surface speciation as a function of time. Additionally, the stability of aged As(V) reacted aluminum oxide was tested via batch desorption experiments to provide some insights on As bioavailability.

Arsenate Desorption

Figures 2 and 3 show total As(V) desorption from aged As(V) reacted aluminum oxide. Since the adsorption kinetics at pH 4.5 were much faster than at pH 7.8 (Fig. 1), the loading levels of the aged samples depended on pH and time (Table 1). Therefore, the amount of desorbed As(V) was normalized with respect to the initial loading levels in Fig. 2 and 3. Continuous As(V) release was observed in all samples at both pHs (Fig. 2 and 3), however the extent of As(V) desorption after 25 replenishment cycles was different in each aged sample. At pH 4.5, total As(V) desorption decreased with increasing aging time from 3 days to 1 year, suggesting a residence time effect (Fig. 2). The extent of As(V) release in 3 day and 1 month aged samples after 15 to 25 days of desorption was much greater than for 4.5 months to 1 year aged samples. Similar residence time effects (i.e., irreversibility) were also observed at pH 7.8 (Fig. 3). In the 3 days and 1 month aged samples, total As(V) release was approximately 80 to 85% after 25 days of desorption; however, only 51 to 56% of As(V) was released from samples aged 4.5 months to 1 year (Fig. 3). Overall, as aging time increased from 3 days to 1 year, the relative amount of As(V) remaining on the mineral surface increased from 23.46 to 54.81% at pH 4.5 and 15.43 to 48.9% at pH 7.8 (Table 1). Stabilization of adsorbed As(V) seems to have occurred after a residence of 4.5 m at both pHs. Similar research findings (i.e., irreversible As(V) desorption from soils and clay minerals) have been reported by several researchers. Woolson and co-workers investigated the aging effects on As(V) extractability from three different Maryland soils (silty clay loam, sandy loam, and fine sand) (Woolson et al., 1971). 1 *M* NH_4Cl extractable As(V) decreased with increasing aging time up to 36 weeks in all soils. Lin and Puls also reported irreversible As(V) sorption on clay mineral surfaces (halloysite, kaolinite, illite, montmorillonite, and chlorite) (Lin and Puls, 2000). Their As(V) recovery decreased with increasing aging time from 1 to 75 days, and the effects were most pronounced in halloysite and kaolinite.

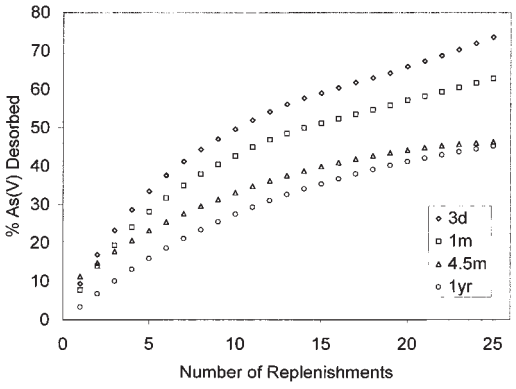

Fig. 2. Residence time effects on As(V) desorption from aged As(V) reacted aluminum oxide at pH 4.5.

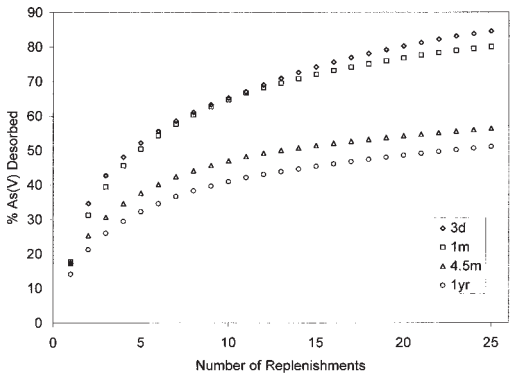

Fig. 3. Residence time effects on As(V) desorption from aged As(V) reacted aluminum oxide at pH 7.8.

Since macroscopic data alone do not provide any mechanistic information (i.e., the changes in the surface speciation over time), we, therefore, performed *in situ* EXAFS analysis on the aged As(V) reacted aluminum oxide samples.

Arsenic K-edge XAS Analysis

Figure 4a shows the background subtracted k^3-weighted χ functions of aged As(V)/aluminum oxide samples and the aluminum arsenate reference compound, mansfieldite. The spectra show

TABLE 1
As(V) desorption experimental conditions and As(V) remaining after 25 days of desorption

Sample	Initial loading levels (μmol m^{-2})	Total As(V) remaining (μmol^{-2}) after 25 replenishment cycles of desorption, (%)
pH 4.5, 3d	2.11	0.56, (23.46%)
pH 4.5, 1m	2.25	0.84, (37.16%)
pH 4.5, 4.5m	2.26	1.24, (54.79%)
pH 4.5, 1yr	2.27	1.24, (54.81%)
pH 7.8, 3d	1.04	0.16, (15.43%)
pH 7.8, 1m	1.13	0.23, (19.98%)
pH 7.8, 4.5m	1.18	0.51, (43.63%)
pH 7.8, 1yr	1.26	0.62, (48.90%)

strong sinusoidal oscillations resulting from O-shell backscattering in all samples. Peak dampening and/or additive amplitude effects in the χ function are also observed as a result of second shell backscattering. However, different experimental conditions (i.e., aging time, loading level, and pH) did not produce any distinctive patterns and shapes in oscillations. Therefore, we Fourier transformed the χ functions to isolate the contribution of neighboring atoms (i.e., As-O and As-Al interatomic distances).

Figure 4b shows the RSFs (uncorrected for phase shift) of aged As(V) adsorption samples at pH 4.5 and 7.8 and mansfieldite. The vertical dashed lines correspond to the As-O and As-Al shells, respectively. The solid lines represent the Fourier Transforms of the experimental data, and the open circles are the theoretical spectra derived from multiple shell fitting. The structural parameters (coordination number (*CN*), the interatomic distance (*R*), and the Debye-Waller factor (σ^2)) obtained from the EXAFS data fitting are pre-

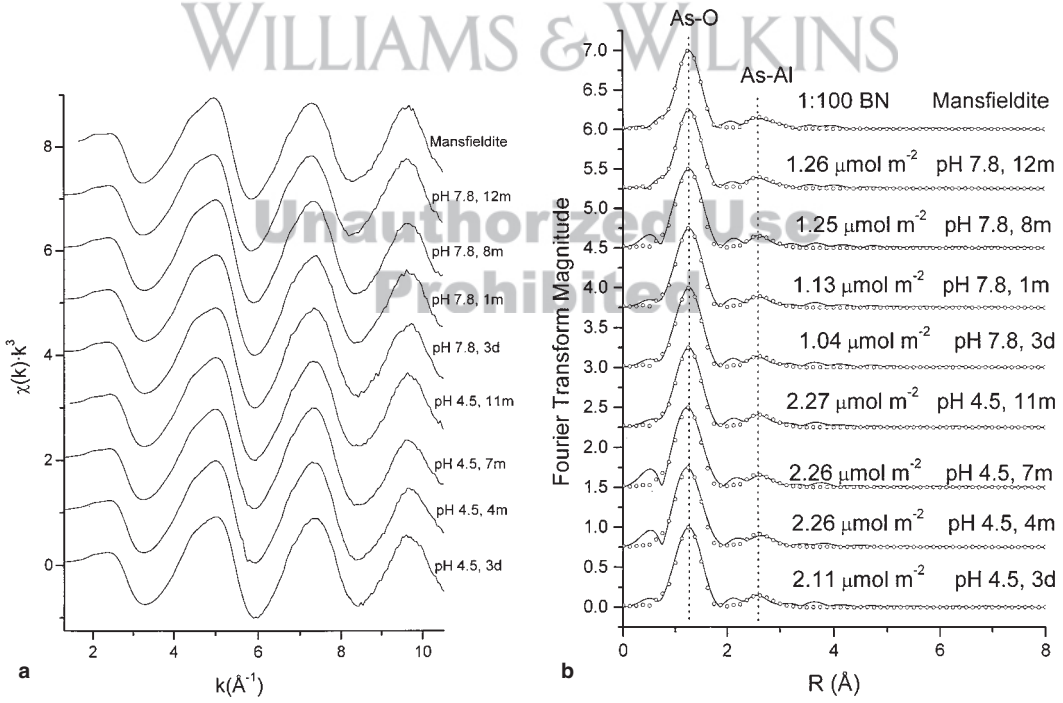

Fig. 4. a. k^3-weighted normalized χ functions for aged As(V) reacted aluminum oxide and reference Al-As(V) compounds. 4b. Fourier transforms of the χ functions (uncorrected for phase shift) for aged As(V) reacted aluminum oxide and reference Al-As(V) compounds. The solid lines are the experimental data and the opened circles represent the theoretical fit to the data.

sented in Table 2. Error estimates of R and N for the As-O shells are ±0.02 Å and ±20%, respectively, based on EXAFS fits on the aluminum arsenate (mansfieldite) reference compound and the values derived from XRD analyses (Harrison, 2000) using ATOMS and FEFF702.

For the first coordination shells, there is good agreement between data derived from EXAFS and X-ray structural refinements. However, slightly large errors exist in R_{As-Al} (±0.13 Å) and N_{As-Al} (±31%), based on the mansfieldite reference compound. The interatomic distances of As-Al derived from EXAFS measurements were much shorter (3.15 Å (EXAFS) vs. 3.28 Å (XRD)). Similar errors have been reported in the case of Zn minerals (O'Day et al., 1998; Ziegler et al., 2001). This observation was explained by (i) the presence of impurities and amorphous compounds (strong disorder neighboring atoms), which strongly influenced the EXAFS analysis, and (ii) different matrices and crystallinity between our materials and the materials used in X-ray analysis (Ziegler et al., 2001).

The As-O radial distances of adsorption samples at both pHs are between 1.68 and 1.70 Å (Table 2), indicating the predominant As (+5) oxidation state (i.e., arsenic tetrahedral; AsO_4) was present at the surface of aluminum oxide regardless of aging time.

The presence of an As-Al shell in all aged samples indicates that As(V) inner-sphere complexation occurs over a residence time of 3 days to 12 months (Fig. 4b and Table 2). The radial distances of As-Al shells ranged from ≈3.11 Å to 3.14 Å. These radial distances can be used to determine the configuration of As(V) inner-sphere complexes forming at the aluminum oxide-water interface. Using a known Al-O distance of the AlO_6 octahedral (1.85–1.97 Å), an O-O edge separation distance of 2.52 to 2.86 Å (Ishizawa et al., 1980), and the experimental As-O distances, the theoretical As-Al bond distances were estimated for different As adsorption configurations (e.g., monodentate mononuclear, bidentate mononuclear, and bidentate binuclear), assuming that the surface structure of γ-Al_2O_3 (i.e., aluminum tetrahedral configuration) was fully converted to the aluminum octahedral configuration of the bayerite polymorph over 1 month of hydration. For monodentate mononuclear inner-sphere complexation, the $R_{As(V)-Al}$ range is calculated to be 3.54 to 3.66 Å. For bidentate mononuclear bonding, the $R_{As(V)-Al}$ range is 2.07 to 2.64 Å. For bidentate binuclear complexation, the $R_{As(V)-Al}$ range is 3.03 to 3.41 Å (Arai et al., 2001). The average As-Al distances of the experimental samples (≈3.11–3.14 Å), are, therefore, consistent with inner-sphere bidentate binuclear As(V) complexes. This configuration is in good agreement with previous equilibrium (<48 h) studies (Arai et al., 2001; Foster et al., 1998).

It is interesting that the As-Al radial distances increase slightly from 3.11 to 3.14 Å with increasing residence time at both pHs (Table 2). This phenomenon could be attributed to the following two different aging mechanisms: (i) a re-

TABLE 2
Structural parameters from EXFAS and XRD analysis for aged As(V) reacted aluminum oxide and aluminum arsenate reference compounds

Sample	As(V)-O			As(V)-Al			
	CN†,¶	R (Å)‡,‖	σ^2(Å^2)§	CN#	R (Å)ᵋ	σ^2(Å^2)	E_o (eV)¶
Mansfieldite	5.07	1.68	0.0031	2.95	3.15	0.006★	3.67
($AlAsO_4$ $2H_2O$)	4	1.68–1.69		4	3.28–3.31		(XRD/FEFF)
Berlinite-like ($AlAsO_4$)	4	1.55–1.56		2	3.15		(XRD/FEFF)
Quartz-like ($AlAsO_4$)	4	1.67		2	3.15–3.16		(XRD/FEFF)
pH 4.5, 3d	5.38	1.68	0.0040	2.60	3.11	0.006★	3.89
pH 4.5, 4m	5.10	1.68	0.0033	2.90	3.12	0.006★	3.22
pH 4.5, 7m	5.14	1.68	0.0037	2.80	3.12	0.006★	3.23
pH 4.5, 11m	5.03	1.68	0.0038	2.71	3.13	0.006★	3.98
pH 7.8, 3d	5.47	1.69	0.0038	2.52	3.11	0.006★	4.05
pH 7.8, 1m	5.51	1.69	0.0040	2.62	3.11	0.006★	4.21
pH 7.8, 7m	5.51	1.69	0.0042	2.78	3.12	0.006★	4.10
pH 7.8, 1yr	5.10	1.70	0.0033	2.65	3.14	0.006★	3.73

†Coordination number. ‡Interatomic distance. §Debye-Waller factor. Fit quality confidence limits for parameters: ¶±20%, ‖±0.02Å, #±31%, and ᵋ±0.13Å. ★Fixed Parameter.

arrangement of surface complexes, and/or (ii) a conversion of surface complexes into aluminum arsenate precipitates.

An increase in the As-Al interatomic distances with aging could occur via a rearrangement of the surface complexes. If a small percentage of bidentate mononuclear complexes (As-Al: 2.07–2.64 Å) were present initially and were gradually converted into bidentate binuclear complexes (As-Al: 3.03–3.41 Å) over time, this would result in an increase in the average As-Al distances.

In addition, the conversion of the surface complexes into aluminum arsenate-like precipitates could result in an increase in the average As-Al radial distance since the increased As-Al radial distances (i.e., 3.12–3.14 Å) are between those of the equilibrium (<48 h) adsorption complexes (3.11 Å) (Arai et al., 2001) and the aluminum arsenate minerals (3.15 Å)(Table-2).

The As-Al distances of As bearing berlinite-like ($AlAsO_4$) and quartz-like ($AlAsO_4$) minerals were estimated using ATOMS and FEFF702 based on X-ray structural refinements (Baumgartner et al., 1989; Thong and Schwarzenbach, 1979). The As-Al distances were the same (i.e., 3.15 Å) in the aluminum tetrahedral minerals (i.e., berlinite-like and quartz-like minerals), but the aluminum octahedral mineral, mansfieldite gave much longer As-Al distances (3.28–3.31 Å) (Table 2). It is possible that residual aluminum tetrahedral molecules of γ-Al_2O_3 could react with arsenate ions to form As bearing berlinite/quartz-like precipitates over time. The intermediate bond distances (3.12–3.14 Å) can be explained if mixtures of adsorption complexes and aluminum arsenate precipitates are present simultaneously. The surface transformation of adsorption complexes to aluminum arsenate-like precipitate phases might occur over time, assuming an increase in As-Al radial distances.

As mentioned above, errors in the As-Al shell in mansfieldite between EXAFS and XRD/FEFF analysis were somewhat large (R_{As-Al} ($\pm$ 0.13 Å) and N_{As-Al} ($\pm$31%)). In the case of berlinite-like and quartz-like minerals, we do not have As-Al distance comparisons between EXAFS and XRD/FEFF analysis. Therefore, it is difficult to make a clear case for the formation of the mansfieldite-like/berlinite-like/quartz-like precipitate in our aged samples based on the parameters derived via EXAFS and XRD analysis alone.

We further investigated the aging mechanisms by comparing XANES spectra of aged adsorption samples and mansfieldite, assuming a three dimensional surface transformation occurred. In Fig. 5a, magnified XANES features occurring at the highest point (≈11.88 keV) after the edge jump show differences between aged samples and mansfieldite. The features (indicted by arrows in Fig. 5a) at pH 4.5 and 7.8 changed with increasing aging time (≥11 m) at both pHs, indicating changes in the local structure. The XANES features in aged (≥11 m) samples seem to be a mixture of mansfieldite and 3 days sorption samples at each pH (Fig. 5a). Therefore, we performed linear combination (LC) analyses of the XANES profile fit on aged (≥11 m) samples between 11.8 and 12.20 keV using XANES spectra of 3 day samples (i.e., bidentate binuclear reference spectra) at each pH and mansfieldite (i.e., an aluminum arsenate precipitate reference spectrum), using the procedure of Pickering et al. (1995). This analysis was done under the assumption that mansfieldite is a good representative of aluminum arsenate precipitates that may form on the aluminum oxide surfaces with aging. Results of the LC fit on ≥11 m samples are shown in Fig. 5b. The percent contribution of mansfieldite was more than 80% in the ≥11 m samples at both pHs. Similarly good fits were obtained in the other intermediate time spectra (1–8 m) (data not shown). The percent contribution of mansfieldite increased from 37% (4 m) to 58% (7 m) at pH 4.5 and from 2% (1 m) to 97% (8 m) at pH 7.8. The trend in increasing contribution of mansfieldite with aging might suggest a surface transformation to aluminum arsenate-like precipitates with aging. However, other aluminum arsenate reference compounds (i.e., As bearing berlinite-like and quartz-like minerals) are not available for the XANES analyses, and we cannot exclude the possibility of berlinite/quartz-like precipitate formation.

During the long-term As(V) adsorption reactions, the total aluminum concentration was less than 100 μmol, and no trends in Al dissolution occurred. The MINEQL$^+$ chemical speciation program (Schecher and McAvoy, 1998) predicted that the system was undersaturated with respect to boehmite, gibbsite, amorphous Al_2O_3, and aluminum arsenate bulk precipitates. Therefore, the aluminum arsenate precipitate can be categorized as a surface precipitate if formed.

Three possible mechanisms can be suggested to explain the surface transformation of adsorption complexes to Al-As(V) surface precipitates. James and Healy suggested that the activity of ions at the mineral-water interface increased as a result of the changes in the dielectric constant properties of the bulk solution (James and Healy,

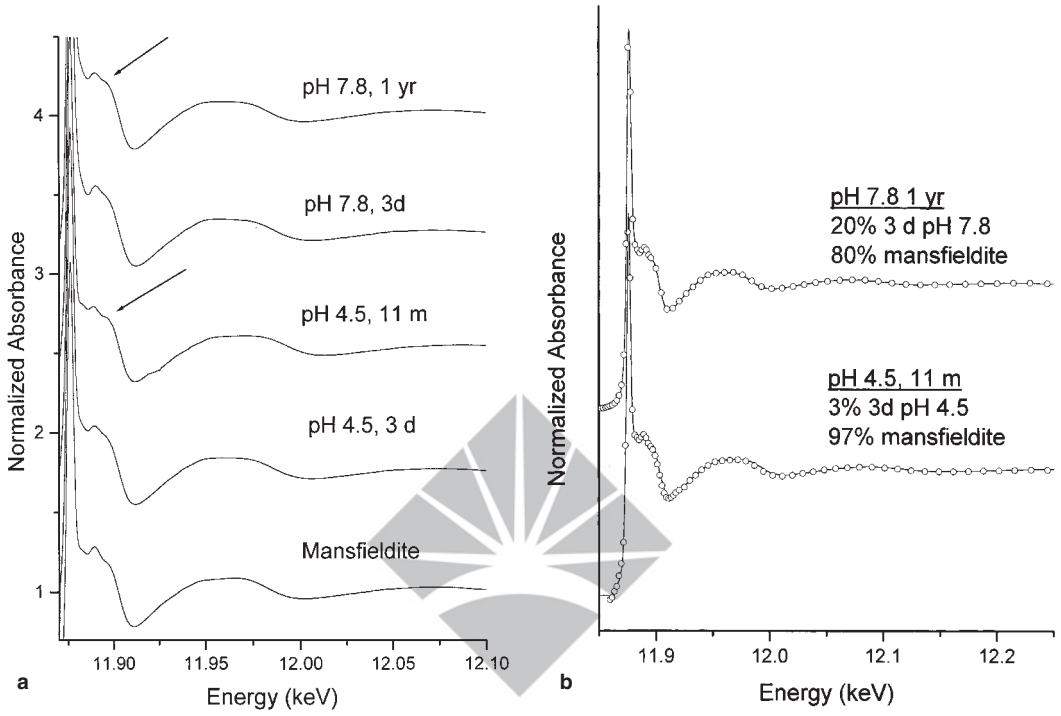

Fig. 5. a. Magnified XANES spectra of aged As(V) sorption samples and mansfieldite. 5b. Results of linear combination (LC) of XANES profile fit for an 11-month aged sample at pH 4.5 and a 1-year aged sample at pH 7.8. The solid lines are the experimental spectra, and the open circles represent the LC fit in which 3d at pH 4.5 or pH 7.8 and mansfieldite spectra were used as components.

1972). Surface precipitation processes can be facilitated by increased ion activity at the interface via decreased dielectric constant of the interface and/or increased ion density near charged surfaces. A second mechanism is that dissolved co-ions from adsorbents and adsorbate ions in the bulk fluid could form co-precipitates at the mineral-water interface (Chisholm-Brause et al., 1990; Farley et al., 1985). Under our experimental conditions at pH 4.5 and pH 7.8, it is possible that ligands (i.e., protons and hydroxyl) promoted aluminum dissolution over time, and the dissolved aluminum ions interacted with nonadsorbed and/or adsorbed arsenate. Nucleation processes gradually result in three-dimensional structures over time. It is true that specific adsorption of inorganic anions (e.g., phosphate and arsenate) can inhibit dissolution of metal oxides (Biber et al., 1994; Bondietti et al., 1993). However, slow dissolution of adsorbents still occurs over time since the mineral/water interface is in disequilibrium with respect to ion transformation. We monitored total Al dissolution during the long term As(V) adsorption. However, there was no trend in dissolved aluminum with increasing As(V) adsorption at both pHs. The final possible mechanism for transformation from adsorption complexes to surface precipitates could be physical entrapment caused by Al oxide particle agglomeration. One could speculate that an initial charge interaction between As(V) nonreacted and reacted aluminum oxide particles can occur with increasing residence time. Since our experimental pHs (4.5 and 7.8) are below the IEP of the aluminum oxide (≈9.3), the surface charge density of As(V) unreacted aluminum oxide particles is positively charged. These positively charged particles could be attracted electrostatically to As(V) adsorbed aluminum oxide surfaces, which are negatively charged because of specific As(V) adsorption. Previous electrophoretic mobility measurements have shown that charge reversal can occur via inner-sphere As(V) surface complexation on aluminum oxides (Arai et al., 2001; Suarez et al., 1999). The particle interaction could eventually lead to the formation of multi-aluminum oxide layers/clusters entrapping adsorption complexes within the structure. Unfortunately, these

surface precipitation mechanisms are still speculative since changes in interfacial physicochemical properties are difficult to measure analytically.

SUMMARY

Biphasic As(V) adsorption was observed at pH 4.5 and 7.8. The kinetics of As(V) adsorption at pH 4.5 was nearly complete in less than 3 days; however, the reaction at pH 7.8 continued over 1 year. As(V) desorption decreased with increasing aging time (3 days–1 yr) at both pHs. Our EXAFS results suggested the presence of inner-sphere bidentate binuclear bonding environments, regardless of aging time; however, changes in the local chemical structure were suggested based on alternations in XANES features on aging. The increased irreversibility of adsorbed As(V) might be caused by changes in the As surface speciation, such as a rearrangement of surface complexes and/or a transformation of surface complexes into aluminum arsenate-like surface precipitates. The residence time effects (i.e., irreversible As(V) adsorption/desorption) could also be ascribed to physicochemical processes. Intraparticle diffusion, sorption reactions on higher energy binding sites (structural defects), and structural entrapment of sorbed As during the particle growth cannot be excluded (Papelis, 1995; Papelis et al., 1995).

Our experimental results can be useful in understanding actual environmental processes (e.g., As reactions in aluminum oxide rich fly coal ash settling ponds) and/or evaluating remediation methods (e.g., alumina as an As(V) uptake coagulant at water treatment plants). Further research on more complex model systems (e.g., competitive organic acid and anion reactions) and in heterogeneous systems (e.g., aluminum oxide rich soils and sediments) is needed to understand better the role of aluminum oxide with respect to As(V) partitioning reactions in soils and sediments.

ACKNOWLEDGMENTS

The authors gratefully acknowledge the DuPont Company for financial contributions to this study and also Drs. R.G. Ford and E.J. Elzinga for helpful discussions. Y.A. appreciates the receipt of a College of Agricultural and Natural Resources Graduate Research Assistantship and expresses gratitude to Dr. Rick Maynard of the DuPont Co. for assistance with BET surface area analysis.

REFERENCES

Allen, H. E., C. P. Huang, G. W. Brailley, and A. R. Bowers. 1995. Metal Speciation and Contamination of Soil. Lewis Publ. Co., Ann Arbor, MI, p. 384.

Anderson, M. A., J. F. Ferguson. and J. Gavis. 1976. Arsenate adsorption on amorphous aluminum hydroxide. J. Colloid Interface Sci. 54:391–399.

Arai, Y., E. J. Elzinga, and D. L. Sparks. 2001. X-ray absorption spectroscopic investigation of arsenite and arsenate adsorption at the aluminum oxide-water interface. J. Colloid Interface Sci. 235:80–88.

Bargar, J. R., G. E. Brown, Jr., and G. A. Parks. 1997. Surface complexation of Pb(II) at oxide-water interfaces: I. XAFS and bond-valence determination of mononuclear and polynuclear Pb(II) sorption products on aluminum oxides. Geochim. Cosmochim. Acta. 61:2617–2637.

Barron, E. A. V., and J. Torrent. 1995. Organic matter delays but does not prevent phosphate sorption by cerrado soils from Brazil. Soil Sci. 159:207–211.

Barrow, N. J., 1974. The slow reactions between soil and anions. 1. Effects of time, temperature, and water content of a soil on the decrease in effectiveness of phosphate for plant growth. Soil Sci. 118:380–386.

Barrow, N. J. 1985. Reactions of anions and cations with variable-charge soils, Adv. Agron. pp. 183–230.

Baumgartner, O., M. Behmer, and A. Preisinger. 1989. The crystal-structure of $AlAsO_4$ at 2 °C, 500 °C and 750 °C. Z. kristallogr. 187: 125–131.

Beek, J., and W. H. van Riemsdijk. 1982. Interactions of orthophosphate ion with soil. *In* Soil Chemistry B, Physico-chemical Models. G.H. Bolt (ed.). Elsevier Sci. Publ. Co., Amsterdam, pp. 259–284.

Biber, M. V., M. D. S. Afonso, and W. Stumm. 1994. The coordination chemistry of weathering: IV. Inhibition of the dissolution of oxide minerals. Geochim. Cosmochim, Acta. 58:1999–2010.

Black, C. A., 1942. Phosphate fixation by kaolinite and other clays as affected by pH, phosphate concentration, and time of contact. Soil Sci. Soc. Am. Proc. 6:123–133.

Bondietti, G., J. Sinniger, and W. Stumm. 1993. The reactivity of Fe(III) (Hydr)oxides: Effects of ligands in inhibiting the dissolution. Colloids Surf. 79: 157–167.

Cheah, S.-F., G. E. Brown, Jr., and G. A. Parks. 1998. XAFS Spectroscopy Study of Cu(II) sorption and amorphous SiO_2 and γ-Al_2O_3: Effect of substrate and time on sorption complexes. J. Colloid Interface Sci. 208:110–128.

Chisholm-Brause, K. F. Hayes, C. J., A. L. Roe, G. E. Brown, Jr., G. A. Parks, and J. O. Leckie. 1990. Spectroscopic investigation of Pb(II) complexes at the γ-Al_2O_3/water interface. Geochim. Cosmochim. Acta. 54:1897–1909.

Colemann, R. 1944. The mechanism of phopsphate fixation by montmorillonitic and kaolinitic clays. Soil Sci. Soc. Am. Proc. 9:72–78.

Cummings, D. E., F. Caccavo, Jr., S. Fendorf, and R. F. Rosenzweig. 1999. Arsenic mobilization by the dissimilatory Fe(III)-reducing bacterium *shewanella alga* BrY. Environ. Sci. Technol. 33:723–729.

Dyer, C., P. J. Hendra, W. Forsling, and M. Ranheimer. 1993. Surface hydration of aqueous gamma-Al_2O_3

studied by Fourier transform raman and infrared spectroscopy. 1. Initial results. Spectrochim. Acta Part A Mol. Biomol. Spectrosc. 49(5–6):691–705.
Edzwald, J. K., D. C. Toensing, and M. C. Leung. 1976. Phosphate adsorption reaction with clay minerals. Environ. Sci. Technol. 10:485–490.
Farley, K. J., D. A. Dzombak, and F. M. M. Morel. 1985. A surface precipitation model for the sorption of cations on metal oxides. J. Colloid Interface Sci. 106:226–242.
Fendorf, S. E., M. J. Eick, P. Grossl, and D. L. Sparks. 1997. Arsenate and chromate retention mechanisms on goethite. 1: Surface structure. Environ. Sci. Technol. 31:315–320.
Ford, R. G., A. C. Scheinost, K. G. Scheckel, and D. L. Sparks. 1999. The link between clay mineral weathering and the stabilization of Ni surface precipitates. Environ. Sci. Technol. 33:3140–3144.
Ford, R. G., and D. L. Sparks. 2000. The nature of Zn precipitates formed in the presence of pyrophyllite. Environ. Sci. Technol. 34:2479–2483.
Foster, A. L., G. E. Brown Jr., T. N. Tingle, and G. A. Parks. 1998. Quantitative arsenic speciation in mine tailing using X-ray absorption spectroscopy. Am. Mineral. 83(5–6):553–568.
Fuller, C. C., J. A. Davis, and G. A. Waychunas. 1993. Surface chemistry of ferrihydrite: Part 2. Kinetics of arsenate adsorption and copreciitation. Geochim. Cosmochim. Acta. 57:2271–2282.
Goldberg, S., and C. T. Johnston. 2001. Mechanisms of arsenic adsorption on amorphous oxides evaluated using macroscopic measurements, vibrational spectroscopy, and surface complexation modeling. J. Colloid Interface Sci. 234:204–216.
Harrison, W. T. A. 2000. Synthetic mansfieldite, $AlASO_4 \cdot 2H_2O$. Acta Crystallogr. Sect. C Cryst. Struct. Commun. 56:E421, part 10.
Hayes, K. F. A. L. Roe, G. E. Brown, Jr., K. O. Hodgson, J. O. Leckie, and G. A. Parks. 1987. In situ x-ray absorption study of surface complexes: Selenium oxyanions on α-FeOOH. Science 238:783–786.
Hingston, F. J., A. M. Posner, and J. P. Quirk. 1974. Anion adsorption by goethite and gibbsite. J. Soil Sci. 25:16–26.
Hsu, P. H., and D. A. Rennie. 1962. Reactions of phosphate in aluminum systems. I. Adsorption of phosphate by x-ray amorphous aluminum hydroxide. Can. J. Soil Sci. 42:197–209.
Ishizawa, N., T. Miyata, I. Minato, F. Marumo, and S. Iwai. 1980. A structural investigation of α-Al_2O_3 at 2170 K. Acta Cryst. Sect. C Cryst. Struct. Commun. 36:228–230.
James, R. O., and T. W. Healy. 1972. Adsorption of hydrolyzable metal ions at the oxide-water interface II. Charge reversal of SiO_2 and TiO_2 colloids by adsorbed Co(II), La(III), and Th(IV) as model systems. J. Colloid Interface Sci. 40:53–64.
Kafkafi, U., A. M. Posner, and J. P. Quirk. 1967. Desorption of phosphate from kaolinite. Soil Sci. Soc. Am. Proc. 31:348–353.
Lin, Z., and R. W. Puls. 2000. Adsorption, desorption and oxidation of arsenic affected by clay minerals and aging process. Environ. Geol. 39:753–759.
Madrid, L., and A. M. Posner. 1979. Desorption of phosphate from goethite. J. Soil Sci. 30:697–707.
O'Day, P., G. A. Parks, and G. E. Brown, Jr. 1994. X-ray absorption spectroscopy of cobalt (II) multinuclear surface complexes and surface precipitates on kaolinite. J. Colloid Interface Sci. 165:269–289.
O'Day, P., S. A. Carroll, and G. A. Waychunas. 1998. Rock-water interactions controlling zinc, cadmium, and lead concentrations in surface waters and sediments, U.S. Tri-state mining district. 1. Molecular identification using X-ray absorption spectroscopy. Environ. Sci. Technol. 32:943–955.
Okajima, H., H. Kubota, and T. Sakuma. 1983. Hysteresis in the phosphorus sorption and desorption processes of soils. Soil Sci. Plant Nutr. 29(3): 271–283.
O'Reilly, S. E., D. G. Strawn, and D. L. Sparks. 2001. Residence time effects on arsenate adsorption/desorption mechanisms on goethite. Soil Sci. Soc. Am. J. 65:67–77.
Papelis, C. 1995. X-ray photoelectron spectroscopic studies of cadmium and selenite adsorption on aluminum oxides. Environ. Sci. Technol. 29:1526–1533.
Papelis, C., and K. F. Hayes. 1996. Distinguishing between interlayer and external sorption sites of clay minerals using X-ray absorption spectroscopy. Colloids Surf. A Physicochem. Eng. Aspects 107: 89–96.
Papelis, C., P. V. Roberts, and J. O. Leckie. 1995. Modeling the rate of cadmium and selenite adsorption on micro- and mesoporous transition aluminas. Environ. Sci. Technol. 29:1099–1108.
Parfitt, R. L. 1979. The nature of the phosphate goethite (α-FeOOH) complex formed with $Ca(H_2PO_4)_2$ at different surface coverage. Soil Sci. Soc. Am. J. 43:623–625.
Parfitt, R. L. 1989. Phosphate reactions with natural allophane, ferrihydrite and goethite. J. Soil Sci. 40:359–369.
Pickering, I. J., G. E. Brown Jr. and T. K. Tokunaga. 1995. Quantitative speciation of selenium in soils using X-ray absorption spectroscopy. Environ. Sci. Technol. 29:2456–2458.
Pignatello, J. J., and B. Xing. 1995. Mechanisms of slow sorption of organic chemicals to natural particles. Environ. Sci. Technol. 30:1–11.
Ressler, T. 1998. Winxas: A program for X-ray absorption spectroscopy data analysis under MS-windows. J. Synch. Rad. 5:118–122.
Ryden, J. C., J. R. Mclaughlin, and J. K. Syers. 1977. Time-dependent sorption of phosphate by soils and hydrous ferric oxides. J. Soil Sci. 28:585–595.
Schecher, W. D., and D. C. McAvoy. 1998. MINEQL+. Environmental Research Software, Hallowell, ME.
Scheckel, K. G., A. C. Scheinost, R. G. Ford, and D. L. Sparks. 2000. Stability of layered Ni hydroxide surface precipitates – a dissolution kinetics study. Geochim. Cosmochim. Acta 64:2727–2735.
Scheidegger, A. M., M. Fendorf, and D. L. Sparks. 1996.

Mechanisms of nickel sorption on pyrophylite: Macroscopic and microscopic approaches. Soil Sci. Soc. Am. J. 60:1763–1772.

Scheidegger, A. M., G. M. Lamble, and D. L. Sparks. 1997. Spectroscopic evidence for the formation of mixed-cation hydroxide phases upon metal sorption on clays and aluminum oxides. J. Colloid Interface Sci. 62:2233–2245.

Sparks, D. L. 1987. Dynamics of soil potassium. Adv. Soil Sci. 6:1–63.

Sparks, D. L. 1989. Kinetics of Soil Chemical Processes. Academic Press, San Diego, CA.

Sparks, D. L., 1995. Sorption phenomena on soils, Environmental soil chemistry. Academic Press, San Diego, CA, pp. 99–139.

Strawn, D. G., A. M. Sheidegger, and D. L. Sparks. 1998. Kinetics and mechanisms of Pb(II) sorption and desorption at the aluminum oxide-water interface. Environ. Sci. Technol. 32:2596–2601.

Suarez, D. L., S. Goldberg, and C. Su. 1999. Evaluation of oxyanion adsorption mechanisms in oxides using FTIR spectroscopy and electrophoretic mobility. *In* Mineral-water Interfacial Reactions Kinetics and Mechanisms. D.L. Sparks and T.J. Grundl (Eds.). American Chemical Society, Washington, DC, pp. 136–178.

Thompson, H. A., G. A. Parks, and G. E. Brown, Jr. 1999. Dynamic interactions of dissolution, surface adsorption, and precipitation in an aging cobalt(II)-clay-water system. Geochim. Cosmochim. Acta. 63(11/12):1767–1779.

Thong, N. G. O., and D. Schwarzenbach. 1979. Use of electric-field gradient calculations in charge-density refinements. 2. Charge-density refinement of the low-quartz structure of aluminum phosphate. Acta Cryst. Sect. A 35:658–664.

USEPA. United States Environmental Protection Agency. 2001. EPA to Implement 10ppb Standard for Arsenic in Drinking Water. EPA. 815-F-01–010.

van Riemsdijk, W. H., F. A. Weststrate, and J. Beek. 1977. Phosphate in soils treated with sewage water: III. Kinetics studies on the reaction of phosphate with aluminum compounds. J. Environ. Qual. 6:26–29.

Waychunas, G. A., B. A. Rea, C. C. Fuller and, J. A. Davis. 1993. Surface chemistry of ferrihydrite: Part 1. EXAFS studies of the geometry of coprecipitated and adsorbed arsenate. Geochim. Cosmochim. Acta 57: 2251–2264.

Wijnja, H., and C. P. Schulthess. 1999. ATR-FTIR and DRIFT spectroscopy of carbonate species at the aged γ-Al_2O_3/water interface. Spectrochim. Acta Part A Mol. Spectrosc. 55:861–872.

Willett, I. R., C. J. Chartres, and T. T. Nguyen. 1988. Migration of phosphate into aggregated particles of ferrihydrite. J. Soil Sci. 39:275–282.

Woolson, E. A., J. H. Axley, and P. C. Kearney. 1971. Correlation between available soil arsenic, estimated by six methods, and response of corn (*Zea Mays* L.). Soil Sci. Soc. Am. Proc. 35:101–105.

Zabinsky, S. I., J. J. Rehr, A. Ankudinov, R. C. Albers, and M. J. Eller. 1995. Multiple-scattering calculations of X-ray-absorption spectra. Physical Review B–Condensed Matter. 52:2995–3009.

Ziegler, F., A. M. Scheidegger, C. A. Johnson, R. Dähn, and E. Wieland. 2001. Sorption mechanisms of zinc to calcium silicate hydrate: X-ray absorption fine structure (XAFS) investigation. Environ. Sci. Technol. 35:1550–1555.